CHEMIJA. 2019. Vol. 30. No. 2. P. 98–107

Formation of ZnO films using the SILAR method

Birutė Šimkūnaitė-Stanynienė*,

Giedrė Grincienė,

Leonas Naruškevičius,

Loreta Tamašauskaitė-Tamašiūnaitė,

Algirdas Selskis,

Vidas Pakštas,

Vitalija Jasulaitienė,

Eugenijus Norkus

Center for Physical Sciences and Technology,
3 Saulėtekio Avenue,
10257 Vilnius, Lithuania

The thin ZnO films were deposited using the successive ionic layer adsorption and reaction (SILAR) method. The morphology, structure and composition of the thin ZnO films were examined using scanning electron microscopy (SEM), X-ray diffraction (XRD) and X-ray photoelectron spectroscopy (XPS). The optical properties of the thin ZnO layers, which were deposited onto glass substrates, were investigated using ultraviolet–visible spectrophotometry (UV/Vis).

It was found that the optical properties of the ZnO films depend on the composition of anionic precursor solutions, which were used for deposition of the ZnO layers. Moreover, the highest band gap energy of 3.86 eV was obtained for the ZnO layer when the 0.026 mol l^{-1} $Na_2B_4O_7$ + 0.002 mol l^{-1} $KMnO_4$ solution was used as the anionic precursor solution for the deposition of ZnO layers.

Keywords: ZnO, SILAR, optical properties

INTRODUCTION

Zinc oxide is an important low-cost and non-toxic semiconductor material with beneficial properties, such as high stability, good optical and electrical characteristics. It is widely used in various applications like gas sensors, transparent conducting oxides, dye sanitised solar cells and buffer layers in $CuInS_2$ solar cells [1–5]. ZnO is an n-type semiconductor with a wide optical band gap at room temperature (3.3 eV) and transparency in the visible range of the solar spectrum [6]. ZnO is very widely used in the optoelectronic and photo catalysis due to its high activity and low cost [7–9].

For deposition of ZnO various physical and chemical methods, such as RF magnetron sputtering [10, 11], spray pyrolysis [12, 13], chemical vapour deposition (CVD) [14], metal organic chemical vapour deposition (MOCVD) [5, 15], sol–gel [16–19], chemical bath deposition (CBD) [20–25], successive ionic layer adsorption and reaction (SILAR) [20, 26–28] and atomic layer deposition (ALD) [29–33], have been used. Chemical methods are attractive because they are simple and do not require complicated expensive arrangements.

This study is focused on the deposition of thin ZnO films by means of the SILAR method. Zn layer was examined. The morphology, structure and composition of the thin ZnO layers were examined using field-emission scanning electron microscopy (FESEM), energy dispersive X-ray analysis (EDX), X-ray photoelectron spectroscopy (XPS) and X-ray diffraction (XRD). The optical properties of the thin ZnO films deposited onto

* Corresponding author. Email: birute.simkunaite@ftmc.lt

the glass substrates were investigated using ultraviolet–visible spectrophotometry (UV/Vis).

EXPERIMENTAL

Chemicals

$Zn(CH_3COO)_2 \cdot 2H_2O$ (Sigma-Aldrich, 99.9%), $Na_2B_4O_7 \cdot 10H_2O$ (Eurochemicals, 99%), $KMnO_4$ (Eurochemicals), H_2O_2 (Merck, 35%), C_2H_5OH (Eurochemicals, 96%) and H_2SO_4 (Chempur, 96%) were of analytical grade and used without further purification. Ultra-pure water with the resistivity of 18.2 MΩ cm^{-1} was used to prepare all the solutions. ITO samples were purchased from Sigma-Aldrich Supply. Standard class microscope glass slides (1.0 × 25 × 75 mm) were used from Citotest Labware Manufacturing Co.

Deposition of the ZnO thin layers by the SILAR method

Prior to the deposition of the ZnO layers, the glass substrates were cleaned with chromic acid, thoroughly rinsed with deionised water and ultrasonicated in C_2H_5OH for 10 min. The indium-tin oxide (ITO) substrates were ultrasonicated in C_2H_5OH for 10 min. Then, the ZnO films were deposited onto the glass or ITO substrates according to the following procedure:

(a) immersion of the glass or ITO substrates into the cationic Zn^{2+} precursor solution for 30 s;

(b) immersion of the treated substrates into one of different anionic precursor solutions listed below for 15 s:

i) 10% vol. of H_2O_2,

ii) 0.026 mol l^{-1} $Na_2B_4O_7$,

iii) 0.026 mol l^{-1} $Na_2B_4O_7$ + 0.002 mol l^{-1} $KMnO_4$;

(c) rinsing of the treated samples with deionized water.

This constitutes one SILAR deposition cycle (N) of the ZnO layer. In this study, the whole cycle described was carried out repeatedly for 10 and 20 times. After that, the samples were dried in the air atmosphere. In addition, the ZnO films deposited onto the glass surface, then $N = 10$ and 20, were annealed in air at 350°C temperature for 30 min.

The cationic Zn^{2+} precursor solution was prepared as follows: at first, 0.052 mol l^{-1} $Na_2B_4O_7$ was mixed with 35% H_2O_2 (10% vol.). Then, the prepared solution was added to the solution containing 0.058 mol l^{-1} $Zn(CH_3COO)_2$. The solution pH was 5.8.

Characterisation of samples

The morphology and composition of the ZnO layers deposited onto the glass or ITO substrates using the SILAR method were characterised using a SEM/FIB workstation Helios Nanolab 650 with an energy dispersive X-ray (EDX) spectrometer INCA Energy 350 X-Max 20. Elemental analysis of the ZnO layers was performed by using an 'ESCALAB MK II' spectrometer (VG Scientific, UK) equipped with a Mg Kα X-ray radiation source (1253.6 eV) operated at 300 W, at a fixed pass energy of 20 eV. The pressure of 1.33×10^{-6} Pa was kept in the UHV analysis chamber. To obtain depth-profiles, the samples were etched in the preparation chamber with ionised argon under vacuum of 5×10^{-4} Pa. The accelerating voltage of ca. 1 kV and the beam current of ~20 μA cm^{-2} were used which corresponded to an etching rate of ~4 nm min^{-1}. Depth-profile spectra were taken after Ar^+ ion sputtering to get a deeper insight into the composition. The XPS spectra were recorded for O1s and $Zn2p_{3/2.}$

XRD patterns of the as-deposited ZnO films on the glass surface ($N = 10$ and 20) and annealed at 350°C temperature in air for 30 min were measured using an X-ray diffractometer SmartLab (Rigaku) equipped with an X-ray tube with a Cu anode. The grazing incidence (GIXRD) method was used in the 2θ range 20–60°. An angle between the parallel beam of X-rays and the specimen surface (w angle) was adjusted to 0.5°. Phase identification was performed using the software package PDXL (Rigaku) and ICDD powder diffraction data-base PDF-4+ (2016 release).

Optical absorption studies of the ZnO layers deposited on the glass substrates were carried out in a wavelength range of 300–800 nm using a UV–VIS spectrophotometer Lambda 35 (Perkin Elmer).

RESULTS AND DISCUSSION

The ZnO films were deposited onto the glass and ITO substrates using the successive ionic layer adsorption and reaction method. The ZnO films were deposited onto the glass or ITO substrates by their immersion into the cationic Zn^{2+} solution (see above) for 30 s, rinsing the treated substrates with ultra-pure water, followed by their immersion into the anionic precursor solution for 15 s and rinsing with ultra-pure water. Herein, the effect of different anionic precursor's solutions on the morphology and properties of the deposited ZnO layers was investigated. Three anionic precursor solutions containing different composition were used: i) 10% vol. of H_2O_2, ii) 0.026 mol l^{-1} $Na_2B_4O_7$ and iii) 0.026 mol l^{-1} $Na_2B_4O_7$ + 0.002 mol l^{-1} $KMnO_4$.

The morphology of the as-grown thin ZnO films was examined by scanning electron microscopy. Figure 1 shows the SEM micrographs under different magnification of the thin ZnO films deposited onto the glass substrate after 10 (a, b) and 20 (c, d) SILAR deposition cycles, using the anionic precursor solution containing 10% vol. of H_2O_2. The SEM micrographs under different magnification of the as-deposited thin ZnO layers onto the ITO substrate by 10 SILAR deposition cycles are given in Fig. 2. The anionic precursor solution was the same. There is no significant visual difference between the morphology of the ZnO films

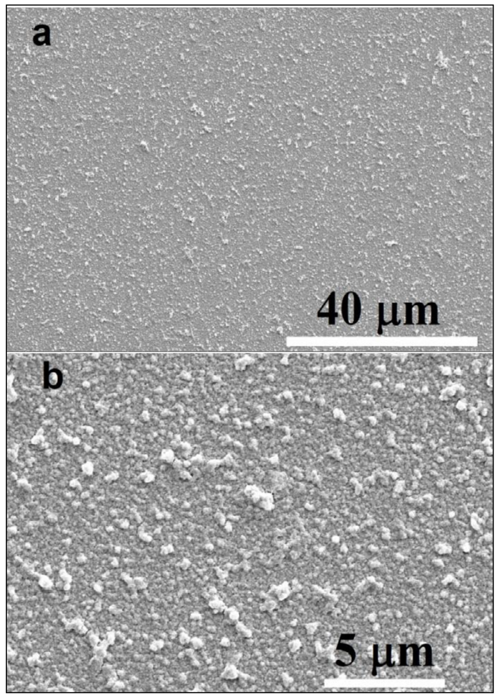

Fig. 2. SEM images under different magnification of the ZnO layer deposited on the ITO sheet after 10 SILAR deposition cycles. 10% vol. H_2O_2 was used as the anionic precursor solution

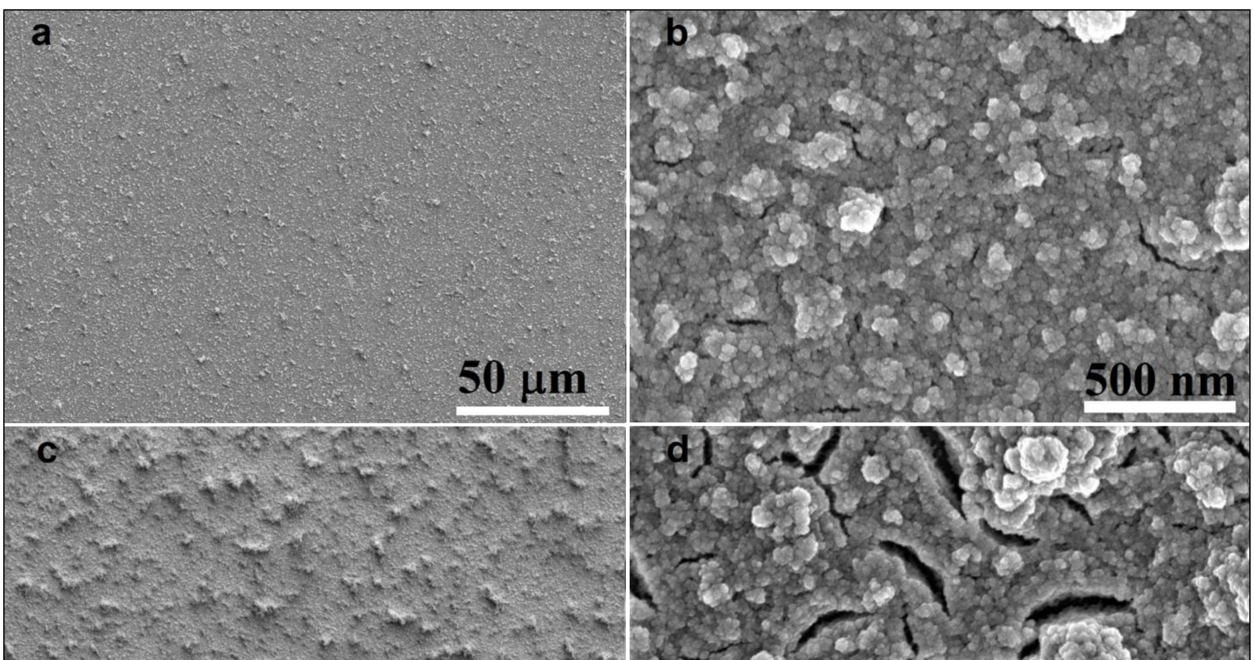

Fig. 1. SEM images under different magnification of the ZnO layer deposited onto the glass sheet after 10 (a, b) and 20 SILAR deposition cycles (c, d). 10% vol. H_2O_2 was used as the anionic precursor solution

deposited onto the glass (Fig. 1) and ITO (Fig. 2) substrates using the anionic precursor solution based on H_2O_2. It is clearly seen that the obtained ZnO films, then *N* = 10, are composed of the ZnO crystallites in size of ca. 25–75 nm (Figs. 1b, 2b). Moreover, the ZnO film deposited on the surface of glass after 20 SILAR deposition cycles was cracked during the sample drying in air (Fig. 1d).

X-ray photoelectron spectroscopy was used to investigate the surface chemical composition of the as-deposited ZnO films onto the ITO surface after 10 SILAR deposition cycles using the anionic precursor solution based on H_2O_2. In order to get a deeper insight into the composition of the modified layer, the XPS spectra of Zn2p and O1s were recorded not only from the sample surface, but also depth-profile spectra were taken after Ar^+ ion sputtering. Figure 3 shows the XP sputter spectra of Zn2p and O1s for the ZnO film deposited onto the ITO surface (*N* = 10) at a depth of ~3 nm (a, b) and ~7 nm (c, d), respectively. The summarised data of XPS analysis of the sample are given in Table 1. As seen from the XPS sputter spectra of Zn2p at a depth of ~3 nm (Fig. 3a) and ~7 nm (Fig. 3c), three peaks at a binding energy (BE) of 1021.71, 1022.54 and 1023.57 eV were identified. Figures 3b and d show the O1s XPS spectra at a depth of ~3 and ~7 nm, respectively. It is clearly seen that the spectra of O1s at a depth of ~3 nm are fitted by three peaks, whereas at a depth of ~7 nm they are fitted by four peaks. The peaks at lower binding energy of 529.86 eV (Fig. 3b) and 530.04–530.90 eV (Fig. 3d) are attributed to the lattice oxygen, e.g. ZnO [34, 35]. Moreover, two

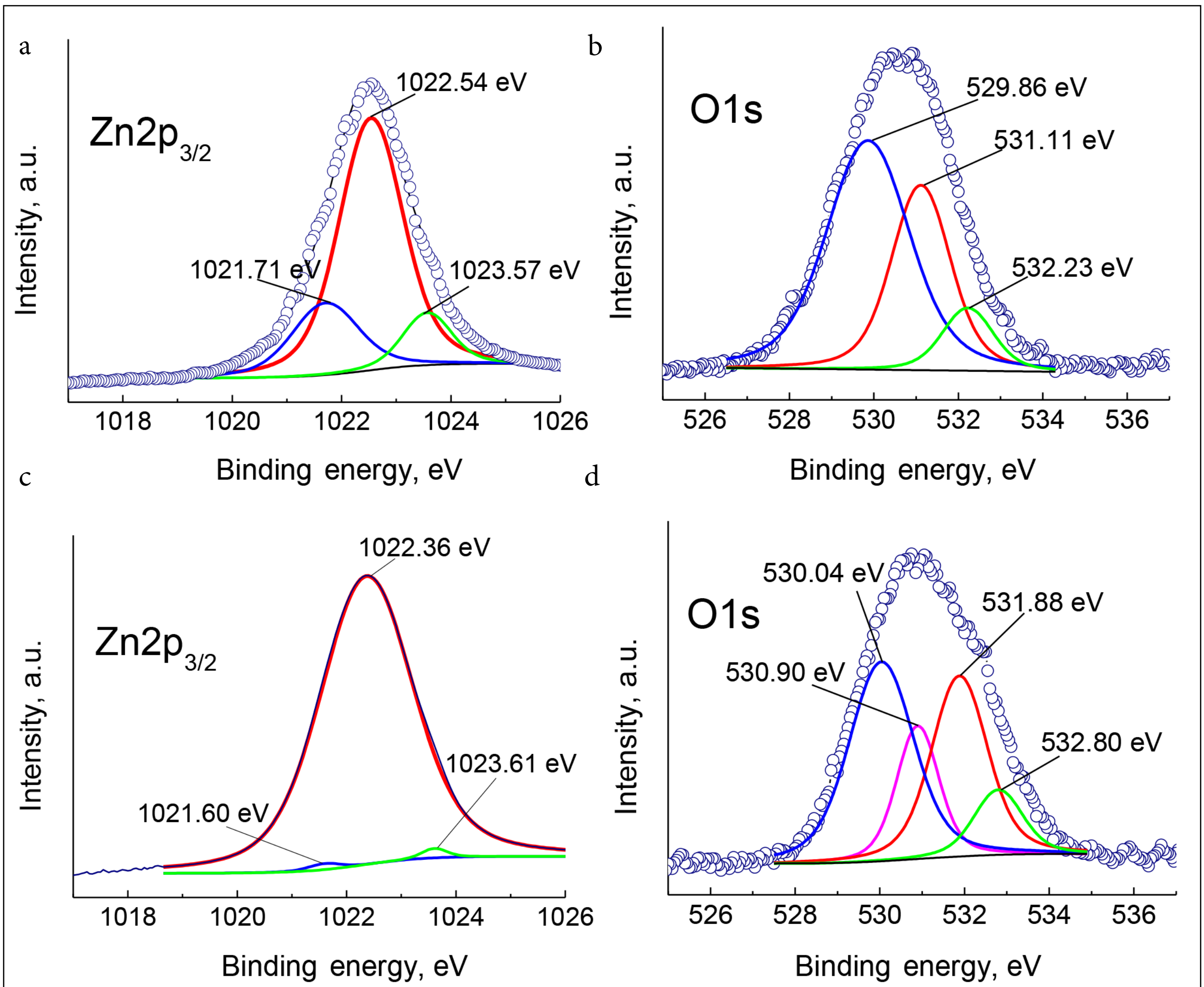

Fig. 3. XPS spectra of Zn2p3/2 (a, c) and O1s (b, d) at a depth of ~3 nm (a, b) and ~7 nm (c, d) for the ZnO layer deposited onto the ITO surface after 10 SILAR deposition cycles. 10% vol. H_2O_2 was used as the anionic precursor solution

layer-related components at ~531.11 and 532.23 eV at a depth of ~3 nm (Fig. 3b) and at ~531.88 and ~532.80 eV at a depth of ~7 nm (Fig. 3d) are well visible in the spectra and can be attributed, respectively, to oxygen–metal (Zn–O) bonding and probably to oxygen on a split-interstitial configuration [36, 37] or oxide near Zn vacancies. From the data in Table 1 it is evident that the integrated intensity at a depth of ~7 nm for the BE peak at 1022.36 eV, which represents the concentration of stoichiometric ZnO, is higher as compared with that at a depth of ~3 nm for BE at 1022.54 eV. Furthermore, the $Zn2p_{3/2}$ spectrum of Zn oxide suffers from an overlap with the metal peak BE. Chemical state determination can be made using the modified Auger parameter ($2p_{3/2}$, $L_3M_{45}M_{45}$) [35]. The Zn $L_3M_{45}M_{45}$ Auger transition spectra for the ZnO layers deposited onto the ITO surface after 10 SILAR deposition cycles have also been recorded at different depths and shown in Fig. 4. As evident, the Zn $L_3M_{45}M_{45}$ Auger peaks at a binding energy of 265.80 eV are characteristic of ZnO (Fig. 4).

Table 1. **XPS data of the elemental composition of the ZnO layer deposited onto the ITO surface after 10 SILAR deposition cycles. The ZnO layers were deposited onto the ITO substrate by its immersion in the cationic Zn^{2+} precursor solution followed by its immersion into the anionic precursor solution containing 10% vol. of H_2O_2**

Depth, nm	Elements			
	Zn2p3		O1s	
	E_b, eV	at.%	E_b, eV	at.%
0 (surface)	1021.63	92.63	530.20	42.30
	1022.78	7.37	531.37	36.86
			532.42	20.84
3	1021.71	20.45	529.86	57.32
	1022.54	68.69	531.11	33.00
	1023.57	10.86	532.23	9.69
7	1021.60	0.72	530.04	40.65
	1022.36	98.39	530.90	17.70
	1023.61	0.89	531.88	31.66
			532.80	10.00
25	1022.48	100	530.87	78.70
			532.09	13.88
			533.09	7.42

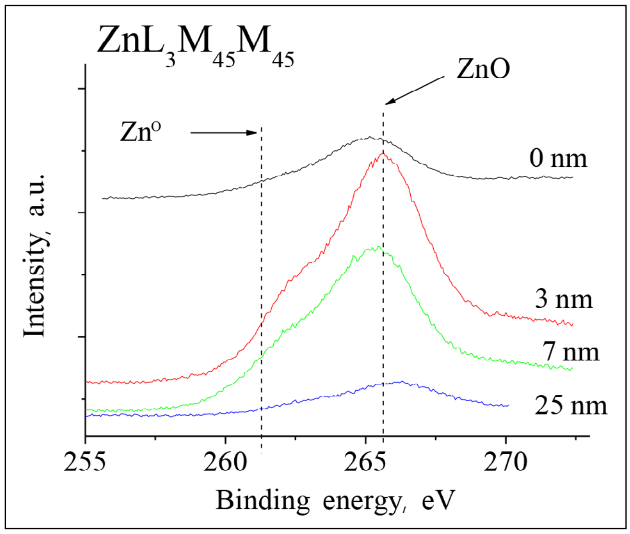

Fig. 4. Zn $L_3M_{45}M_{45}$ Auger electron spectra at a different depth for the ZnO layer deposited onto the ITO surface after 10 SILAR deposition cycles. 10% vol. H_2O_2 was used as the anionic precursor solution

The main peak of Zn (LMM) Auger transition occurs at 987.50 eV kinetic energy (KE) [38, 39]. From this value and $Zn2p_{3/2}$ binding energy, we calculated the modified Auger parameter α' according to Eq. (1) [40]:

$$\alpha' = BE_{Zn2p_{3/2}} + KE_{Zn\ LMM}. \quad (1)$$

A lower α' indicates a lower electron density at the atom, i.e. a higher oxidation state [41]. The calculated values of the α-parameter from the $Zn2p_{3/2}$ and LMM spectra are 2010.28, 2010.04, 2009.86 and 2010.00 eV at a depth of 0, 3, 7 and 25 nm, respectively, and clearly demonstrate that ZnO has formed in the film [35].

The structure and crystallinity of the ZnO layers deposited onto the glass surface and annealed at 350°C temperature for 30 min were investigated by the X-ray diffraction method. Figure 5 presents the XRD patterns of the annealed ZnO layers, which were deposited on the glass surface after 10 (a) and 20 (b) SILAR deposition cycles using the anionic precursor solution containing 10% vol. of H_2O_2. It was found that the ZnO films annealed in air at 350°C temperature for 30 min have a hexagonal structure with a slightly deformed lattice (PDF 01-79-5604) (Fig. 5). Diffraction peaks observed in the patterns confirm that the ZnO films have a hexagonal (wurtzite) structure.

The ZnO layers were also deposited on the glass sheet using the anionic precursor solutions

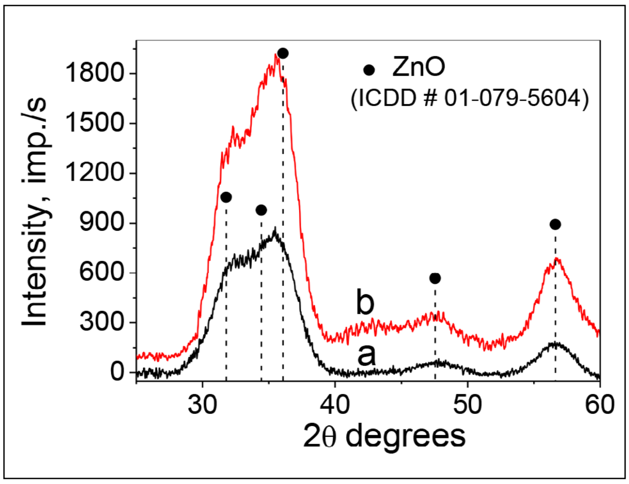

Fig. 5. XRD patterns of the ZnO layers deposited on the glass surface after 10 (a) and 20 (b) SILAR deposition cycles and annealed in air at 350°C for 30 min. 10% vol. H_2O_2 was used as the anionic precursor solution

containing 0.026 mol l^{-1} $Na_2B_4O_7$ + 0.002 mol l^{-1} $KMnO_4$ or 0.026 mol l^{-1} $Na_2B_4O_7$. In order to cover completely the glass surface with the ZnO layers, 20 SILAR deposition cycles were used.

Figure 6 presents the SEM images of the ZnO layer deposited onto the glass sheet after 20 SILAR deposition cycles using the anionic precursor solutions containing 0.026 mol l^{-1} $Na_2B_4O_7$ + 0.002 mol l^{-1} $KMnO_4$ (a) and 0.026 mol l^{-1} $Na_2B_4O_7$ (b). As seen from the data in Fig. 6, the deposited ZnO layer is even, but of poorer quality than that obtained using the anionic 10% vol. H_2O_2 precursor solution (Fig. 1). The composition of the ZnO films deposited on the glass surface after 20 SILAR deposition cycles using the anionic precursor solution containing 0.026 mol l^{-1} $Na_2B_4O_7$ + 0.002 mol l^{-1} $KMnO_4$ was examined by XPS. The summarised data are given in Table 2. Figure 7 shows the XP sputter spectra of Zn2$p_{3/2}$ (a) and O1s (b) for the same sample at a depth of ~3 nm. As evident, the Zn2$p_{3/2}$ spectra at a depth of ~3 nm (Fig. 7a) are fitted by two peaks, whereas the O1s spectra are fitted to four peaks. The Zn2$p_{3/2}$ lines for ZnO are quoted at 1021.44 eV with the O1s for ZnO found at 530.21 eV (Table 2) [22, 23].

The optical properties of the ZnO layers deposited onto the glass sheet were investigated by means of ultraviolet–visible spectrophotometry. The UV/Vis absorption spectra were recorded in a wavelength range of 300–800 nm at room temperature.

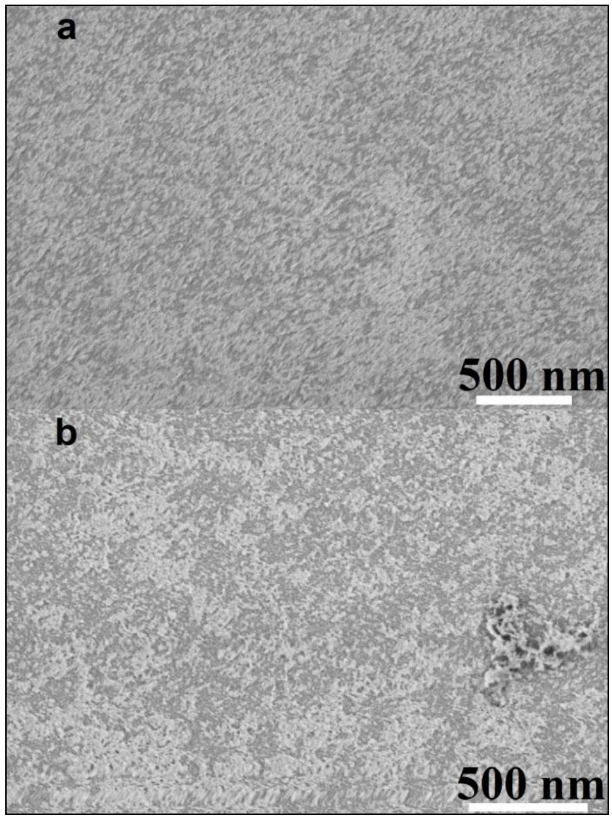

Fig. 6. SEM images of the ZnO layer deposited on the glass sheet after the 20 SILAR deposition cycles using the anionic precursor solution containing 0.026 mol l^{-1} $Na_2B_4O_7$ + 0.002 mol l^{-1} $KMnO_4$ (a) and 0.026 mol l^{-1} $Na_2B_4O_7$ (b)

Table 2. **XPS data of the elemental composition of the ZnO layer deposited onto the glass surface after 20 SILAR deposition cycles. The ZnO layers were deposited onto the glass surface by its immersion in the cationic Zn^{2+} precursor solution followed by its immersion into the anionic precursor solution containing 0.026 mol l^{-1} $Na_2B_4O_7$ + 0.002 mol l^{-1} $KMnO_4$**

Depth, nm	Elements			
	Zn2p3		O1s	
	E_b, eV	at.%	E_b, eV	at.%
0 (surface)	1019.73	0.80	530.61	5.80
	1021.77	18.60	532.42	36.30
	1022.78	5.40	533.40	3.70
	1023.88	1.90	534.07	4.40
3	1021.44	15.60	530.21	8.30
	1023.13	1.40	531.33	11.50
			532.53	31.80
			533.74	5.10

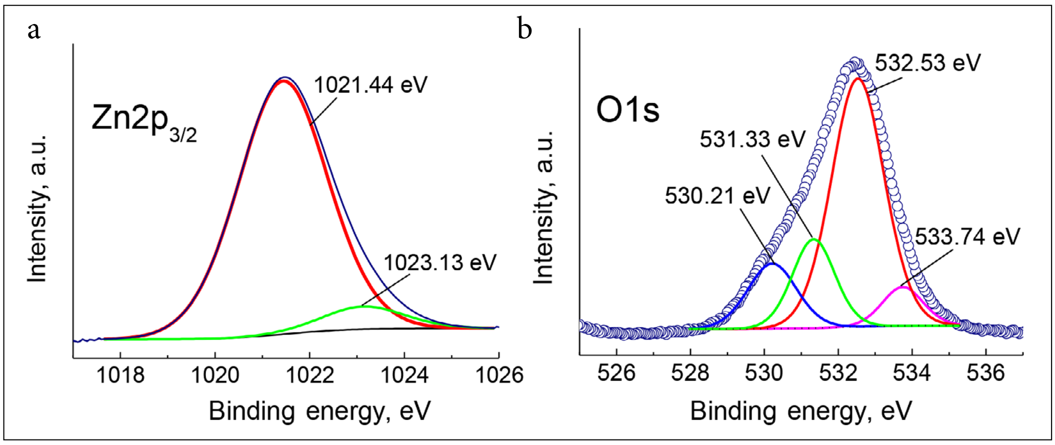

Fig. 7. XPS spectra of $Zn2p_{3/2}$ (a) and O1s (b) at a depth of ~3 nm for the ZnO layer deposited on the glass surface after 10 SILAR cycles. As the anionic precursor a solution containing 0.026 mol l^{-1} $Na_2B_4O_7$ + 0.002 mol l^{-1} $KMnO_4$ was used

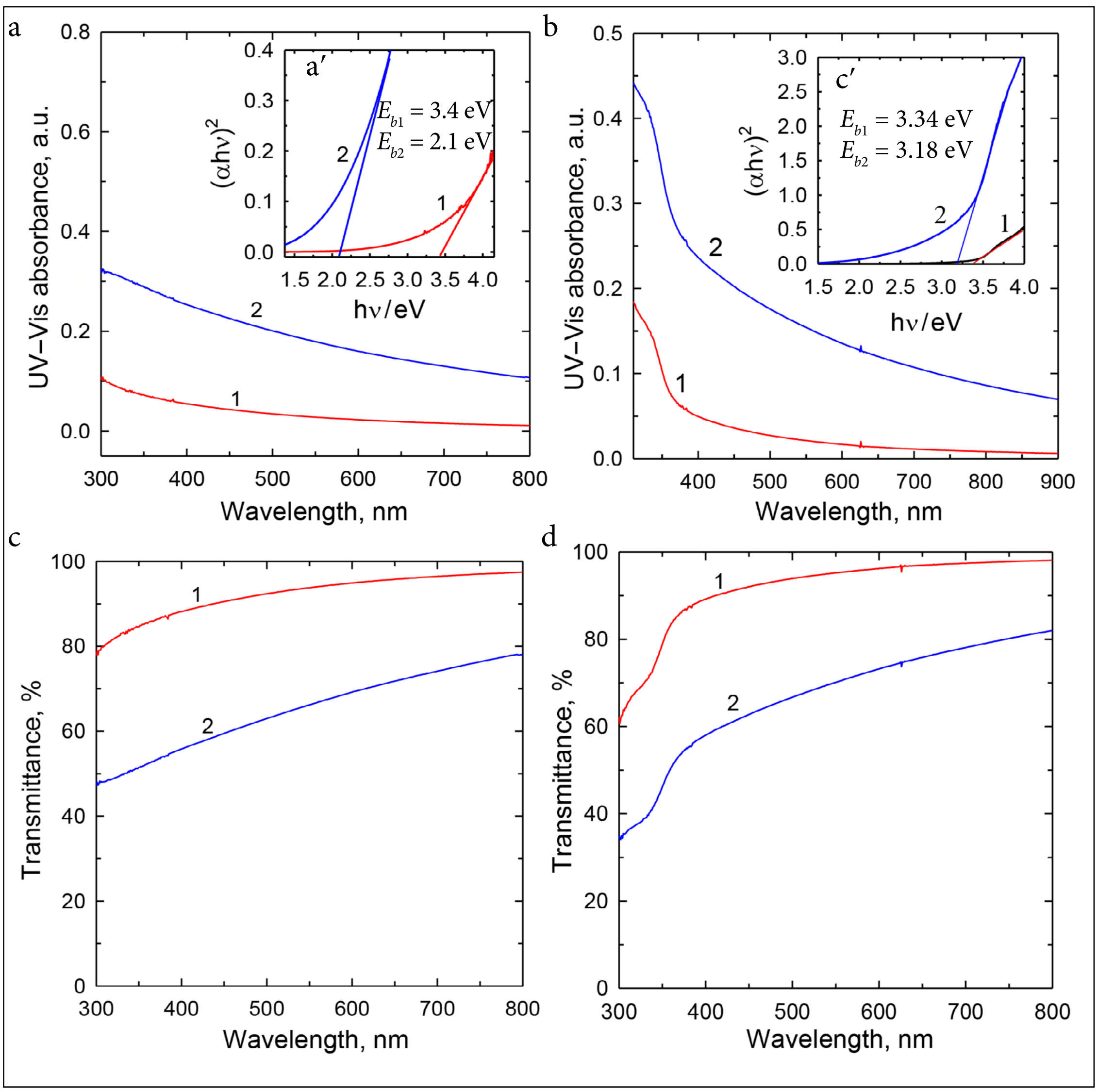

Fig. 8. UV–Vis absorption spectra (a, as deposited; c, annealed) and transmittance spectra (b, as-deposited; d, annealed) of the ZnO layer deposited on the glass surface after 10 (1) and 20 (2) SILAR deposition cycles. 10% vol. H_2O_2 was used as the anionic precursor solution. The inset (a′, as-deposited; c′, annealed) represents the dependence of $(\alpha h\nu)^2$ on hν

Figure 8 shows the optical absorption spectra and transmittance spectra for the as-deposited (a, b) and annealed at 350°C (c, d) ZnO films, which were prepared using 10% vol. H_2O_2 as the anionic precursor solution. In addition, the ZnO films were as-grown on the glass surface using 10 (1) and 20 (2) SILAR deposition cycles (Fig. 8). The UV–Vis absorption and transmittance spectra for the as-grown ZnO films after 20 SILAR deposition cycles using the 0.026 mol l^{-1} $Na_2B_4O_7$ + 0.002 mol l^{-1} $KMnO_4$ or 0.026 mol l^{-1} $Na_2B_4O_7$ solutions as the anionic precursor ones are given in Fig. 9. As evident from the data in Fig. 8 (b, d), the as-grown and annealed ZnO films, which were prepared using 10% vol. H_2O_2 as the anionic precursor solution (N = 10), exhibit a higher transparency in the visible range as compared with those obtained using 20 SILAR deposition cycles. After 10 SILAR deposition cycles, the transparency of the both as-deposited and annealed ZnO films is close to 100%, while after 20 SILAR deposition cycles the one is about 60% (Fig. 8b, d). In the case of the as-grown ZnO films (N = 20) obtained from two different anionic precursor solutions that were composed of 0.026 mol l^{-1} $Na_2B_4O_7$ + 0.002 mol l^{-1} $KMnO_4$ or 026 mol l^{-1} $Na_2B_4O_7$ solutions revealed almost the same transparency of ~100% (Fig. 9b).

In order to confirm the nature of optical transition in all samples, the obtained data were analysed using the classical absorption equation known as Tauc equation [30]:

$$\alpha = \alpha_o (h\nu - E_g)^n / h\nu. \tag{2}$$

Here α_o is a constant, $h\nu$ is the incident photon energy, E_g is the separation between the bottom of the conduction band and the top of the valence band and n is the constant. For the allowed direct transition n = 1/2, and for the allowed indirect transition n = 2. The plot of $(ah\nu)^2$ versus $h\nu$ for the ZnO film as-deposited on the glass substrate by its immersion into the cationic Zn^{2+} precursor solution followed by its immersion into the anionic precursor solution containing 10% vol. of H_2O_2 is shown in the inset a' of Fig. 8a. As evident, the ZnO films deposited using 10 and 20 SILAR deposition cycles have a band gap energy of 3.40 eV (E_{b1}) and 2.10 eV (E_{b2}), respectively (Fig. 8a'). The obtained results are in good agreement with the optical bang gap energy found for ZnO bulk – 3.30 eV [6]. After annealing of the samples in air at 350°C temperature for 30 min, the band gap energy values were equal to 3.34 eV ($E_{b1'}$) and 3.18 eV ($E_{b2'}$) when the ZnO films were deposited using 10 and 20 SILAR deposition cycles, respectively (Fig. 8c'). Notably, the higher bind energies of 3.84 and 3.86 eV were obtained for the as-grown ZnO films (N = 20), using the solutions containing 0.026 mol l^{-1} $Na_2B_4O_7$ + 0.002 mol l^{-1} $KMnO_4$ or 0.026 mol l^{-1} $Na_2B_4O_7$ as the anionic precursor ones, respectively (Fig. 9a).

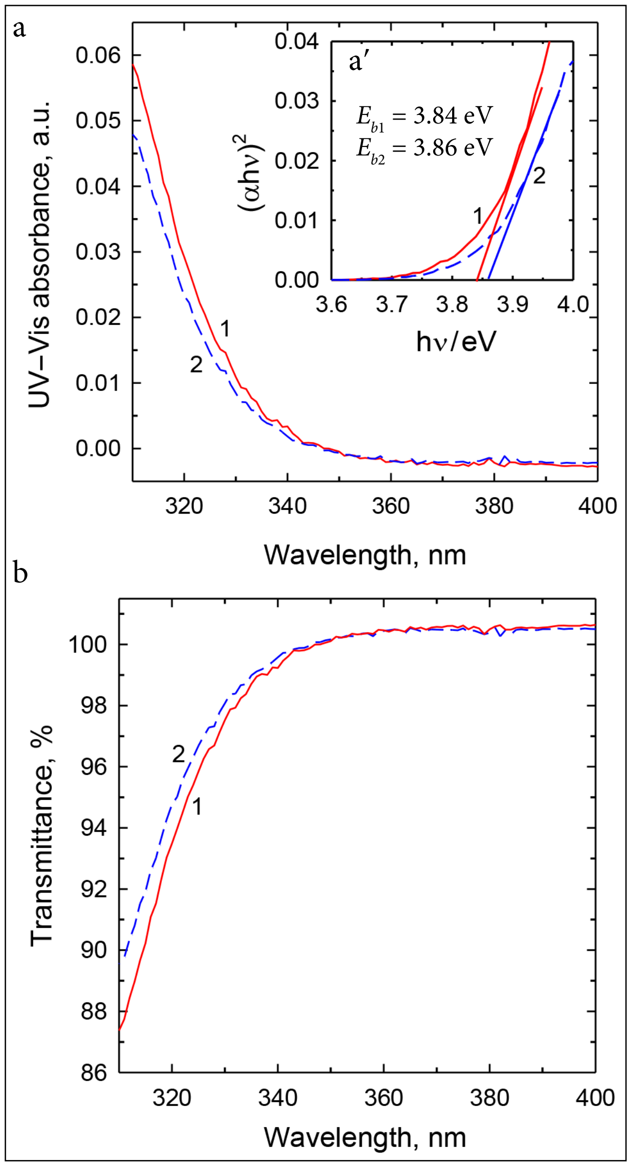

Fig. 9. (a) UV–Vis absorption spectra and (b) transmittance spectra of the ZnO layer deposited on the glass surface after 20 SILAR deposition cycles. As the anionic precursor solutions containing 0.026 mol l^{-1} $Na_2B_4O_7$ + 0.002 mol l^{-1} $KMnO_4$ (1) and 0.026 mol l^{-1} $Na_2B_4O_7$ (2) were used. The inset (a') represents the dependence of (αhν)2 on hν

CONCLUSIONS

The thin ZnO films were deposited onto the glass and ITO substrates using the successive ionic layer adsorption and reaction method (SILAR). The effect of different anionic precursor solutions on the morphology and optical properties of the ZnO films has been investigated.

It has been found that the optical properties of the as-grown ZnO films depend on the composition of the anionic precursor solutions, which were used for the deposition of the latter films. The as-grown ZnO films have a band gap energy varied from 2.10 to 3.86 eV. Moreover, the highest band gap energy of 3.86 eV was obtained for the as-grown ZnO film when the 0.026 mol l^{-1} $Na_2B_4O_7$ + 0.02 mol l^{-1} $KMnO_4$ solution was used as the anionic precursor. The transparency of the ZnO films was ~100% when the anionic precursor solutions containing 10% vol. H_2O_2 (N = 10), 0.026 mol l^{-1} $Na_2B_4O_7$ + 0.002 mol l^{-1} $KMnO_4$ (N = 20) or 0.026 mol l^{-1} $Na_2B_4O_7$ (N = 20) were used. However, the 100% transparency was obtained for the annealed ZnO films, which were prepared by using 10% vol. H_2O_2 (N = 10) as the anionic precursor solution.

ACKNOWLEDGEMENTS

The work was carried out within the project VP1-3.1-ŠMM-08-K-01-009 that is partly supported by the National Program ‘An Improvement of the Skills of Researchers’ launched by the Lithuanian Ministry of Education and Science.

Received 19 March 2019
Accepted 1 April 2019

References

1. D. Wu, K. Cao, F. Wang, et al., *Chem. Eng. J.*, **280**, 441 (2015).
2. J. Park, D. S. Shin, D.-H. Kim, *J. Alloys Compd.*, **611**, 157 (2014).
3. X. S. Zhou, J. Zhang, R. Hou, et al., *Appl. Surf. Sci.*, **315**, 307 (2014).
4. V. R. Shinde, T. P. Gujar, C. D. Lokhande, et al., *J. Cryst. Growth*, **296**, 6 (2006).
5. S. Pati, P. Banerji, S. B. Majumder, *Sens. Actuators, A*, **213**, 52 (2014).
6. V. Srikant, D. R. Clarke, *J. Appl. Phys.*, **83**, 5447 (1998).
7. M. Guo, A. Ng, F. Liu, et al., *J. Phys. Chem. C*, **115**, 11095 (2011).
8. Y. Liu, H. Liu, Y. Yu, et al., *Mater. Lett.*, **143**, 319 (2015).
9. W. Zheng, R. Ding, X. Yan, G. He, *Mater. Lett.*, **201**, 85 (2017).
10. A. Purohit, S. Chander, A. Sharma, et al., *Opt. Mater.*, **49**, 51 (2015).
11. K. Cicek, T. Karacali, H. Efeoglu, et al., *Sens. Actuators, A*, **260**, 24 (2017).
12. A. Bedia, F. Z. Bedia, M. Aillerie, et al., *Energy Procedia*, **74**, 529 (2015).
13. V. Mata, A. Maldonadas, M. Olvera, *Mater. Sci. Semicon. Proc.*, **75**, 288 (2018).
14. L. Fanni, B. A. Aebersold, D. T. L. Alexander, et al., *Thin Solid Films*, **565**, 1 (2014).
15. X.-L. Chen, X. Yang, J.-M. Liu, et al., *Vacuum*, **109**, 74 (2014).
16. L. Znaidi, *Mater. Sci. Eng., B*, **174**, 18 (2010).
17. M. Xin, L.Z. Hu, D.-P. Liu, et al., *Superlattices Microstruct.*, **74**, 234 (2014).
18. L. Znaidi, T. Chauveau, A. Tallaire, *Thin Solid Films*, **617**, 156 (2016).
19. U. Chaitra, D. Kekuda, K. Mohan Rao, *Ceram. Int.*, **43**, 7115 (2017).
20. S. B. Jambure, S. J. Patil, A. R. Deshpande, et al., *Mater. Res. Bull.*, **49**, 420 (2014).
21. C. D. Lokhande, P. M. Gondkar, R. S. Mane, et al., *J. Alloys Compd.*, **475**(**1–2**), 304 (2009).
22. V. R. Shinde, C. D. Lokhande, R. S. Mane, et al., *Appl. Surf. Sci.*, **245**(**1–4**), 407 (2005).
23. K. V. Gurav, U. M. Patil, S. M. Pawar, et al., *J. Alloys Compd.*, **509**, 7723 (2011).
24. F. V. Molefe, L. F. Koao, B. F. Dejene, H. C. Swart, *Opt. Mater.*, **46**, 292 (2015).
25. Y. Qu, X. Huang, Y. Li, et al., *J. Alloys Compd.*, **698**, 719 (2017).
26. C. Vargas-Hernández, F. N. Jiménez-García, J. F. Jurado, et al., *Microelectron. J.*, **39**, 1347 (2008).
27. P. V. Rajkumar, K. Ravichandran, M. Baneto, et al., *Mater. Sci. Semicon. Process.*, **35**, 189 (2015).
28. S. Fairose, S. Ernest, *Physica B*, **557**, 63 (2019).
29. A. Mauro, M. Cantarella, G. Nicotra, et al., *Appl. Catal., B*, **195**, 68 (2016).
30. D. Pal, J. Singhal, A. Mathur, et al., *Appl. Surf. Sci.*, **421**, 341 (2017).
31. S. Kim, S. Lee, S.-Y. Ham, et al., *Appl. Surf. Sci.*, **469**, 804 (2019).
32. T. N. Walter, S. Lee, X. Zhang, et al., *Appl. Surf. Sci.*, **480**, 43 (2019).
33. H. Frankenstein, C. Z. Leng, M. D. Losego, et al., *Org. Electron.*, **64**, 37 (2019).
34. [http://www.xpsfitting.com/].
35. M. C. Biesinger, L. W. M. Lau, A. R. Gerson, et al., *Appl. Surf. Sci*, **257**, 887 (2010).
36. P. Erhart, A. Klein, K. Albe, *Phys. Rev. B*, **72**, 085213 (2005).

37. A. G. Joshi, S. Sahai, N. Gandhi, et al., *Appl. Phys. Lett.*, **96**, 123102 (2010).
38. D. Briggs, M. P. Seach, *Surface Analysis by Auger and X-ray Photoelectron Spectroscopy*, Mir, Moscow (1987).
39. A. M. Chaparo, C. Maffiotte, M. T. Gutierrez, et al., *Thin Solid Films*, **431–432**, 373 (2003).
40. C. D. Wagner, W. M. Riggs, L. E. Davis, et al., *Handbook of X-ray Photoelectron Spectroscopy*, Perkin-Elmer Corporation, Minnesota (1978).
41. M. Krzywiecki, L. Grzadziel, A. Sarfraz, et al., *Phys. Chem. Chem. Phys.*, **17**, 10004 (2015).
42. J. Tauc, R. Grigorovici, A. Vancu, *Phys. Status Solidi B*, **15(2)**, 627 (1966).

Birutė Šimkūnaitė-Stanynienė, Giedrė Grincienė, Leonas Naruškevičius, Loreta Tamašauskaitė-Tamašiūnaitė, Algirdas Selskis, Vidas Pakštas, Vitalija Jasulaitienė, Eugenijus Norkus

ZnO DANGŲ FORMAVIMAS SILAR METODU

Santrauka

ZnO dangos buvo nusodinamos ant stiklo ir indžio alavo oksido (ITO) paviršių, taikant pasikartojantį joninio sluoksnio adsorbijos ir reakcijos (SILAR) metodą. Nusodintų plonų ZnO dangų morfologija, struktūra ir sudėtis buvo tiriamos pasitelkus skenuojančiąją elektronų mikroskopiją (SEM), rentgeno spindulių difrakciją (XRD) ir rentgeno fotoelektronų spektroskopiją (XPS), o optinės savybės – UV/Vis spektrofotometriją.

Nustatyta, kad ZnO dangų, nusodintų ant stiklo paviršiaus, optinės savybės priklauso nuo anijoninių pirmtakų tirpalų, naudojamų ZnO sluoksniams nusodinti, sudėties. Didžiausia ZnO dangų E_b yra 3,86 eV, kai dangų nusodinimui anijoniniu tirpalu buvo pasirinktas 0,026 mol l^{-1} $Na_2B_4O_7$ + 0,002 mol l^{-1} $KMnO_4$ tirpalas. Be to, ZnO dangų pralaidumas buvo ~100 %, kai jos nusodintos panaudojant anijoninius tirpalus: 10 % H_2O_2, 0,026 mol l^{-1} $Na_2B_4O_7$ + 0,002 mol l^{-1} $KMnO_4$ arba 0,026 mol l^{-1} $Na_2B_4O_7$.